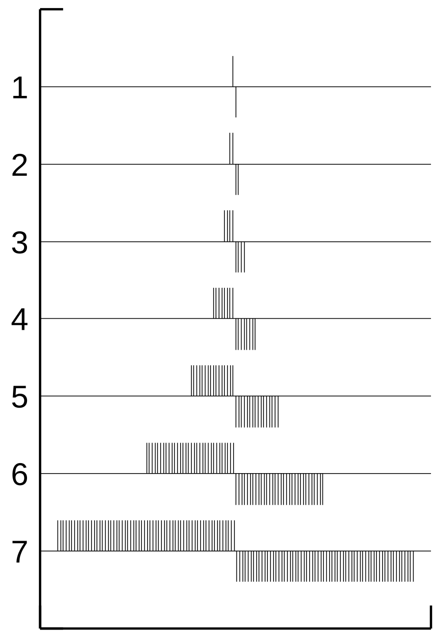

Figure 1. Haar wavelet filters for scales $\tau_j = 2^{j-1}$, $j = 1, 2, \ldots, 7$.

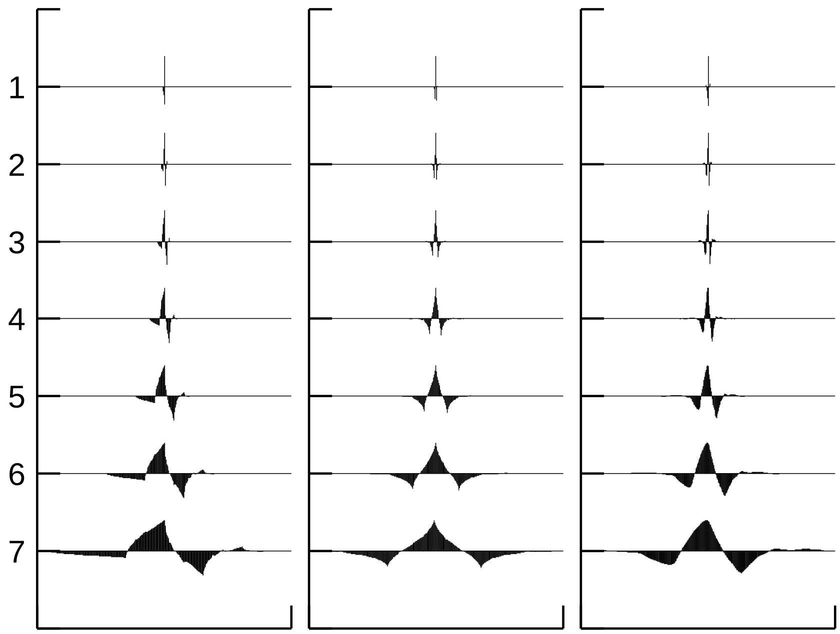

Figure 2. D(4), C(6) and LA(8) wavelet filters for scales $\tau_j = 2^{j-1}$, $j = 1, 2, \ldots, 7$.

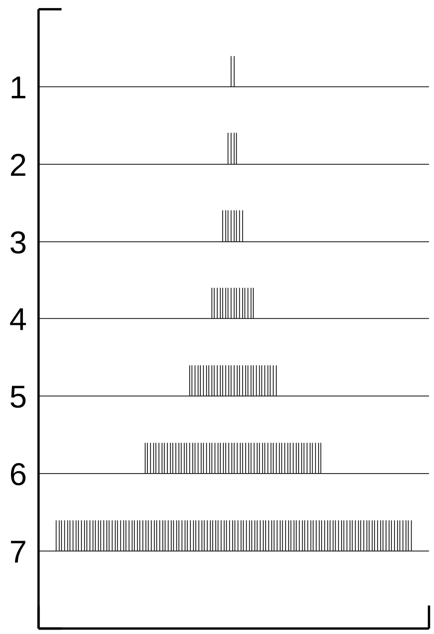

Figure 3. Haar scaling filters for scales $\lambda_{J_0} = 2^{J_0},\ J_0 = 1, 2, \ldots, 7$.

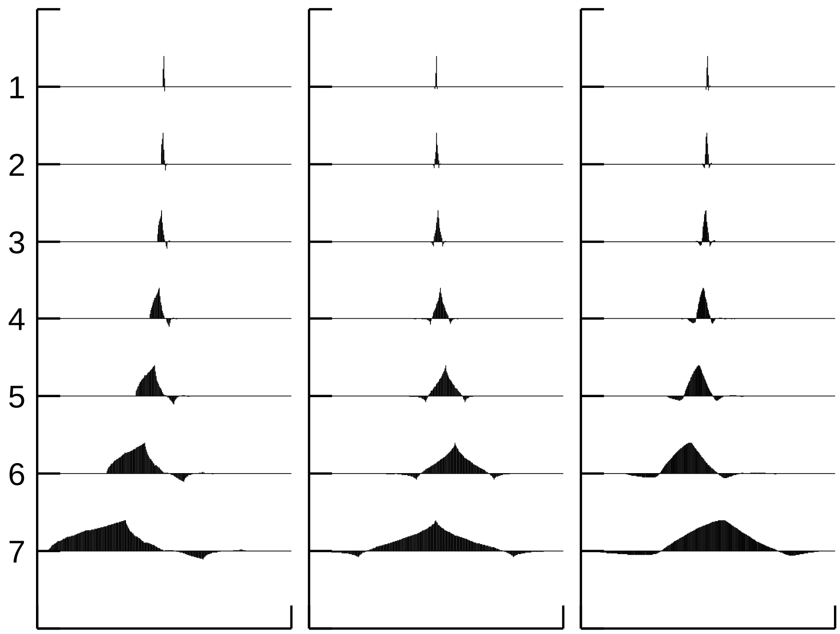

Figure 4. D(4), C(6) and LA(8) scaling filters for scales $\lambda_{J_0} = 2^{J_0}$, $J_0 = 1, 2, \ldots, 7$.

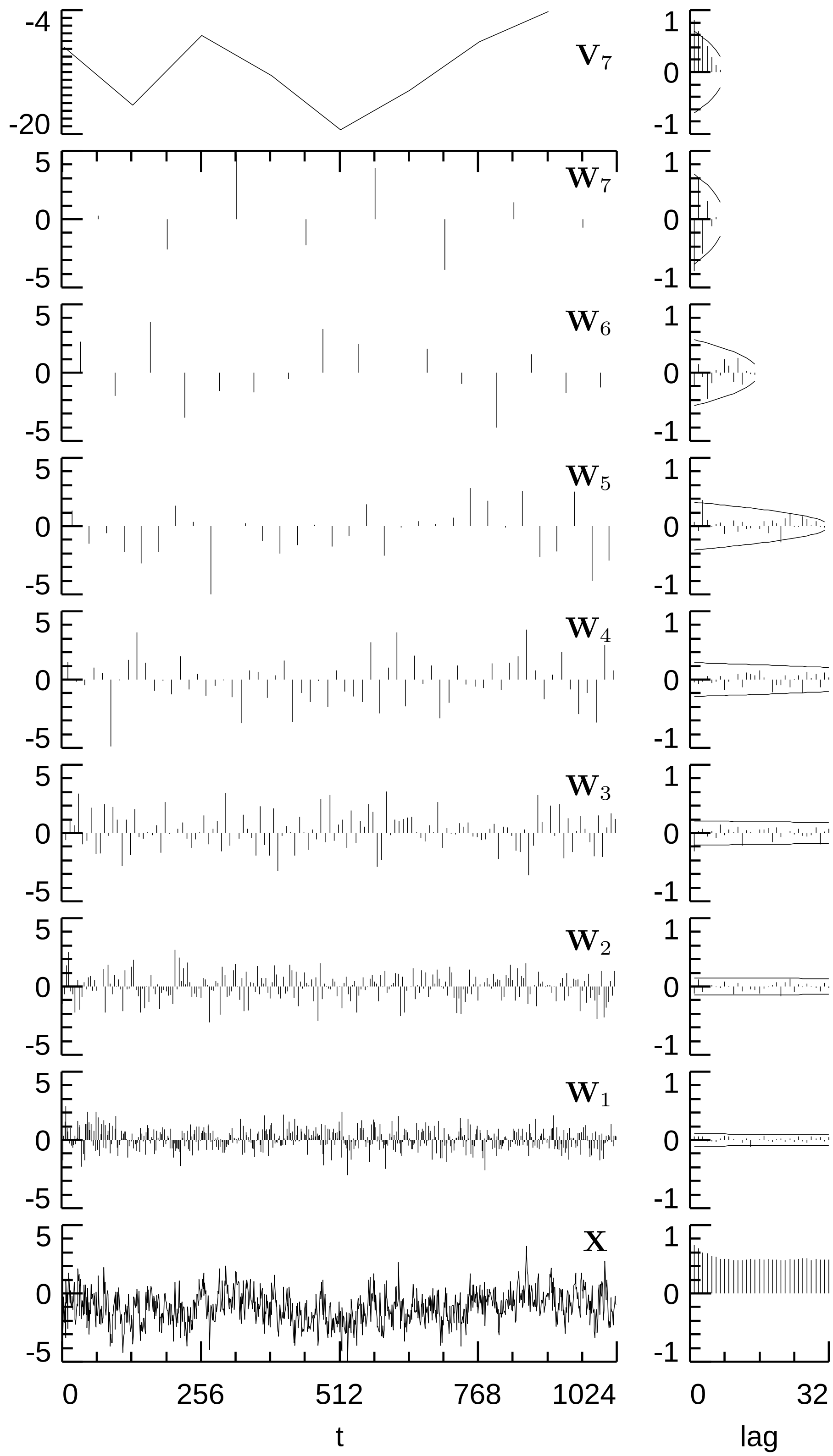

Figure 5. LA(8) DWT coefficients for simulated FD(0.4) time series and sample ACSs.

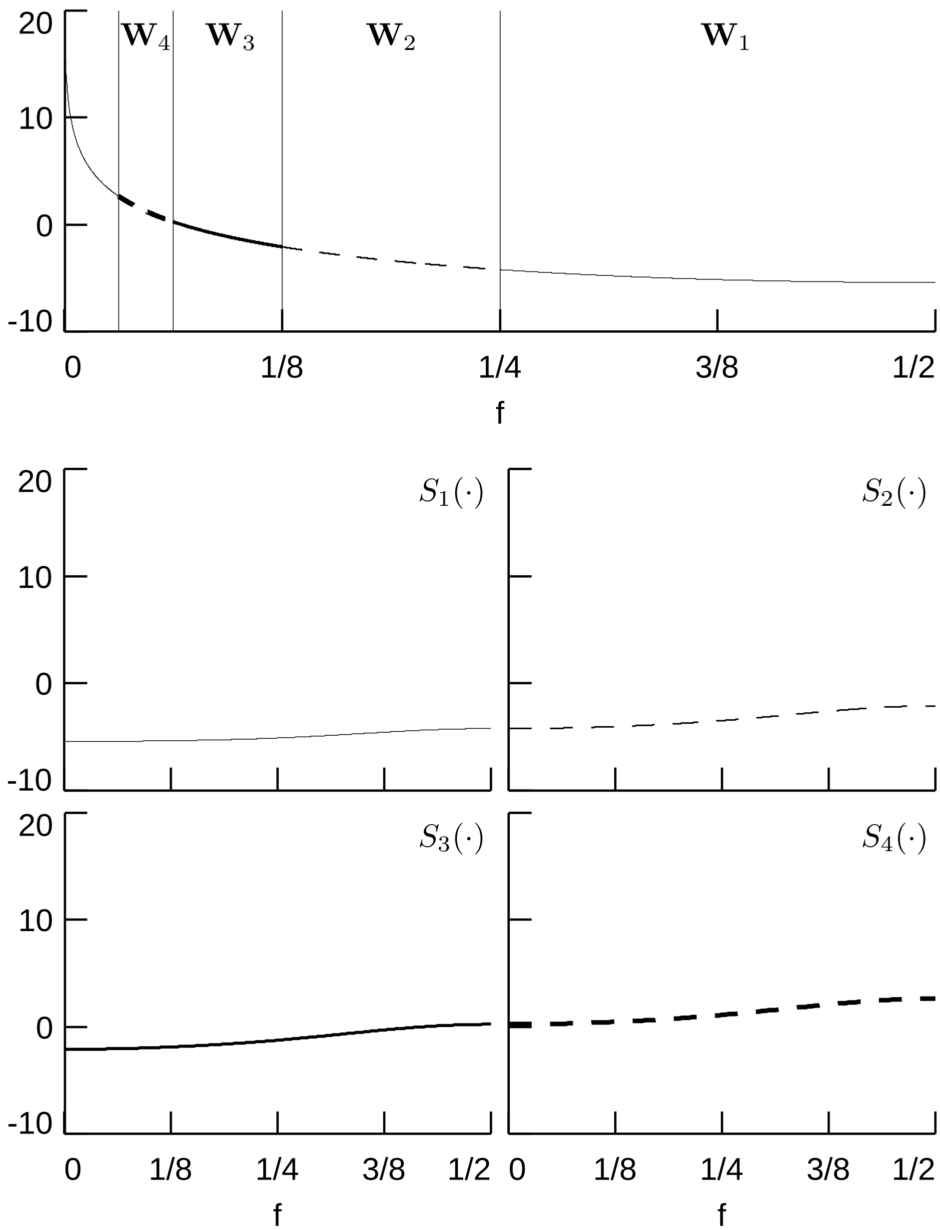

Figure 6. SDFs for an FD(0.4) process (top plot) and for nonboundary LA(8) wavelet coefficients in $\mathbf{W}_1$, $\mathbf{W}_2$, $\mathbf{W}_3$ and $\mathbf{W}_4$. The vertical axes are all in units of decibels (i.e., we plot $\log_{10}(S_X(f))$ versus f). The vertical lines in the top plot denote the nominal pass-bands for the four $\mathbf{W}_j$.

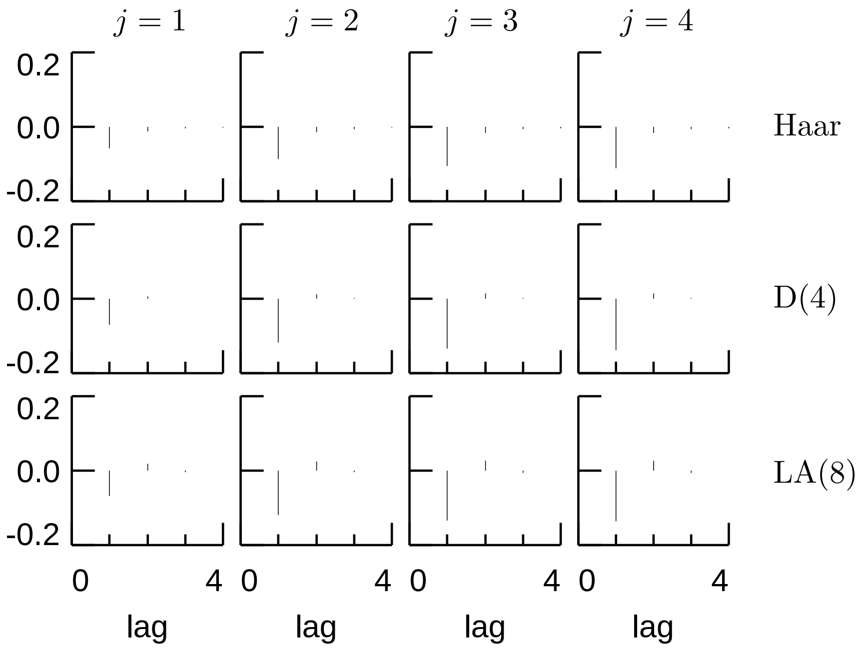

Figure 7. ACSs at $\tau = 1, \ldots 4$ for Haar, D(4) and LA(8) wavelet coefficients $W_{j,t}$, $j = 1, \ldots 4$, of an FD(0.4) process. The ACS values are plotted as deviations from zero (some are not visible because they are so close to zero).

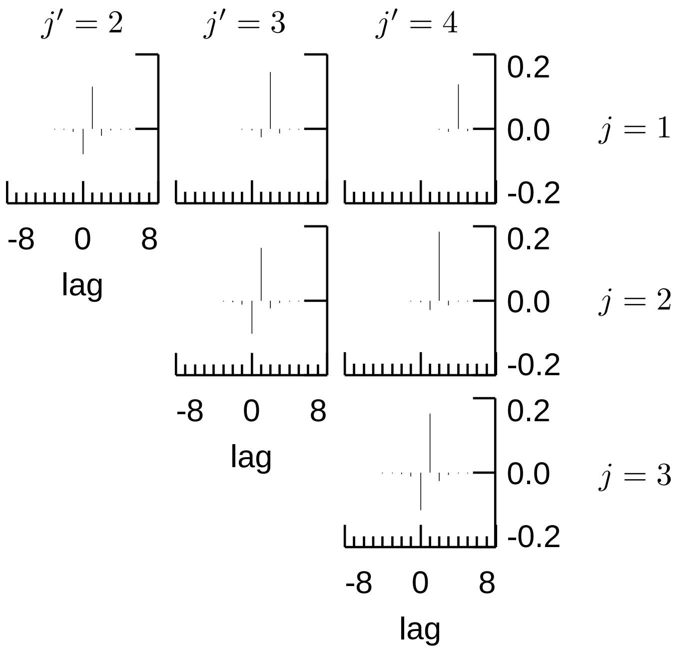

Figure 8a. Correlation between the Haar wavelet coefficients $W_{j,t}$ and $W_{j',t'}$ formed from an FD(0.4) process and for levels satisfying $1 \le j < j' \le 4$.

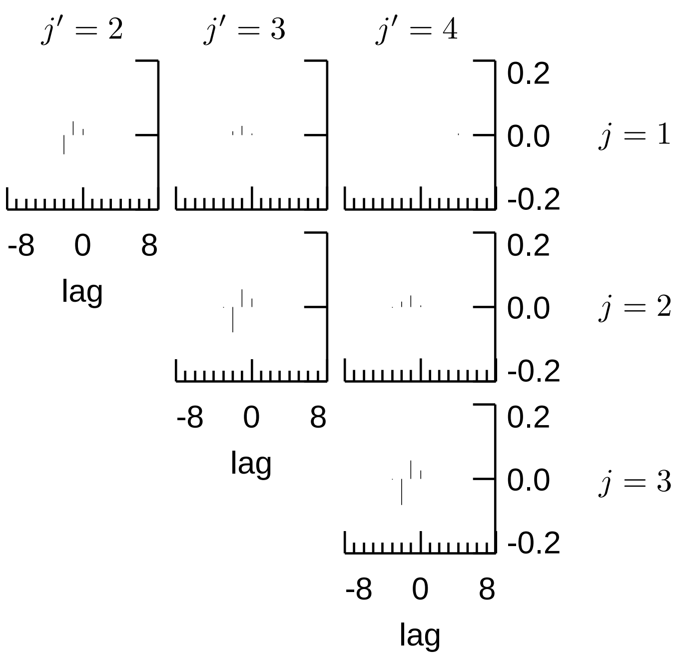

Figure 8b. As in Figure 8a, but now using the LA(8) DWT.

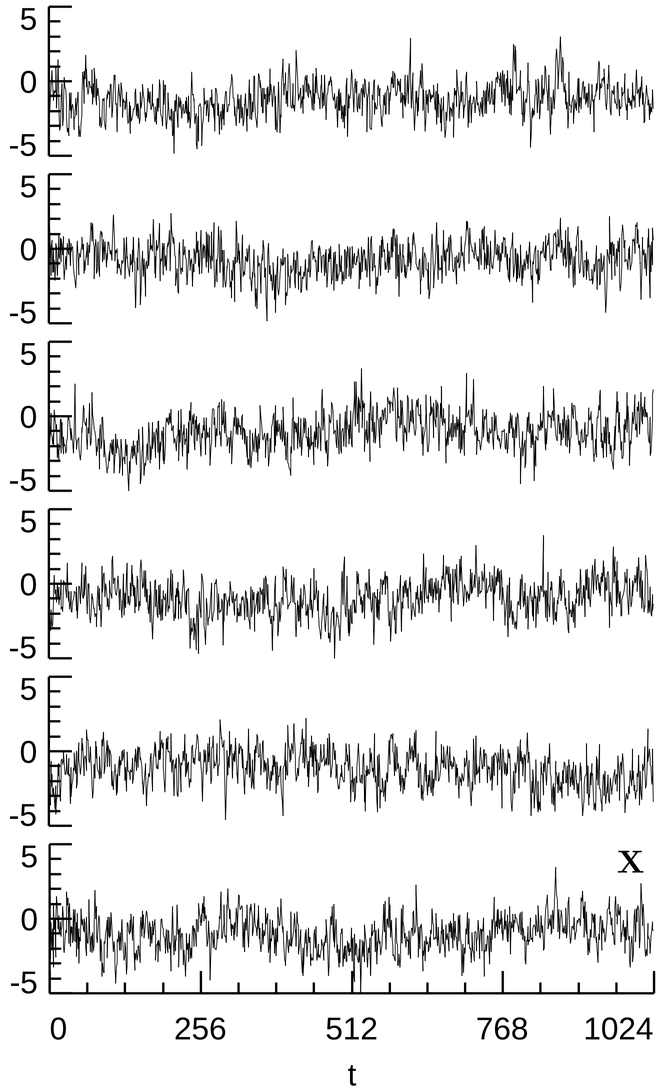

Figure 9. Simulated FD(0.4) time series $\mathbf{X}$ of Figure 5 (bottom panel), abovw which are five series that were bootstrapped from $\mathbf{X}$ using an LA(8) DWT.

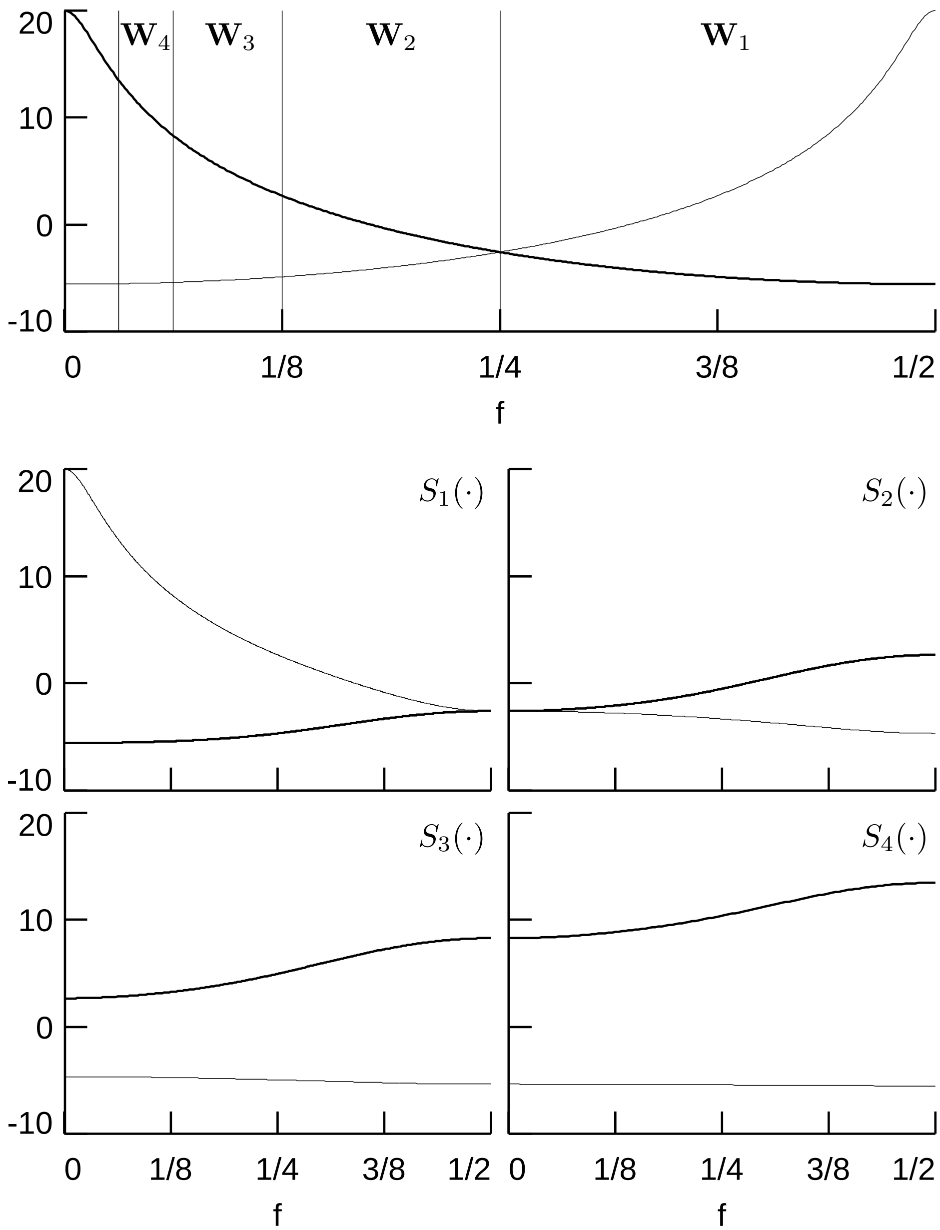

Figure 10. SDFs for AR(1) processes (top plot) with $\phi = 0.9$ (thick curve) and -0.9 (thin) and for corresponding nonboundary LA(8) wavelet coefficients in $\mathbf{W}_1$ to $\mathbf{W}_4$ (bottom four plots). The vertical axes are in decibels, and the vertical lines in the top plot denote the nominal pass-bands for the four $\mathbf{W}_j$.

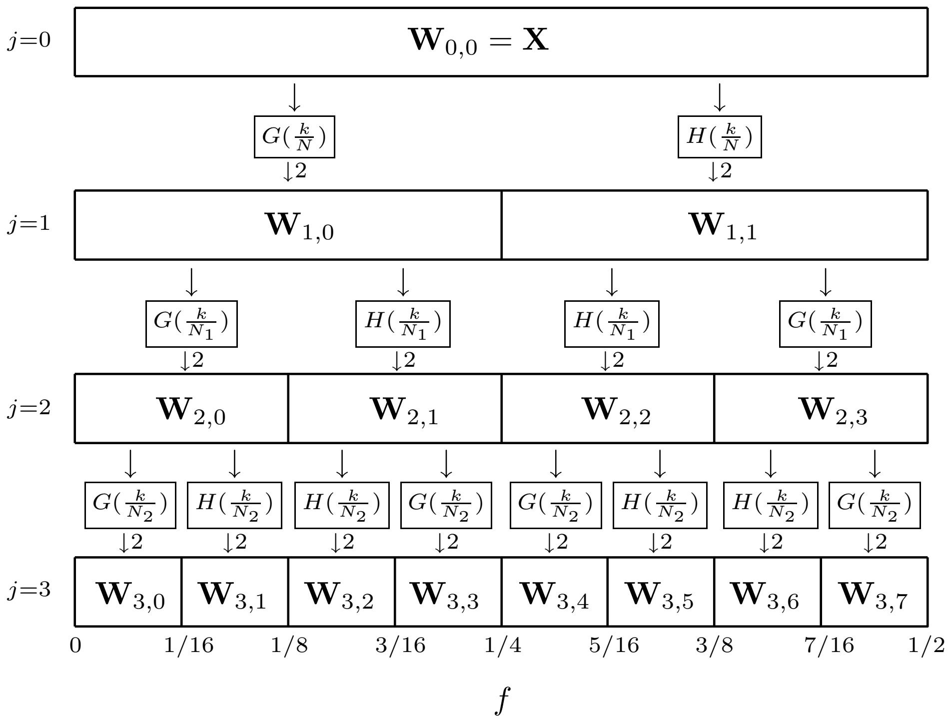

Figure 11. Flow diagram illustrating the analysis of $\mathbf{X}$ into $\mathbf{W}_{3,0}, \ldots, \mathbf{W}_{3,7}$ (recall that $N_j \equiv N/2^j$).

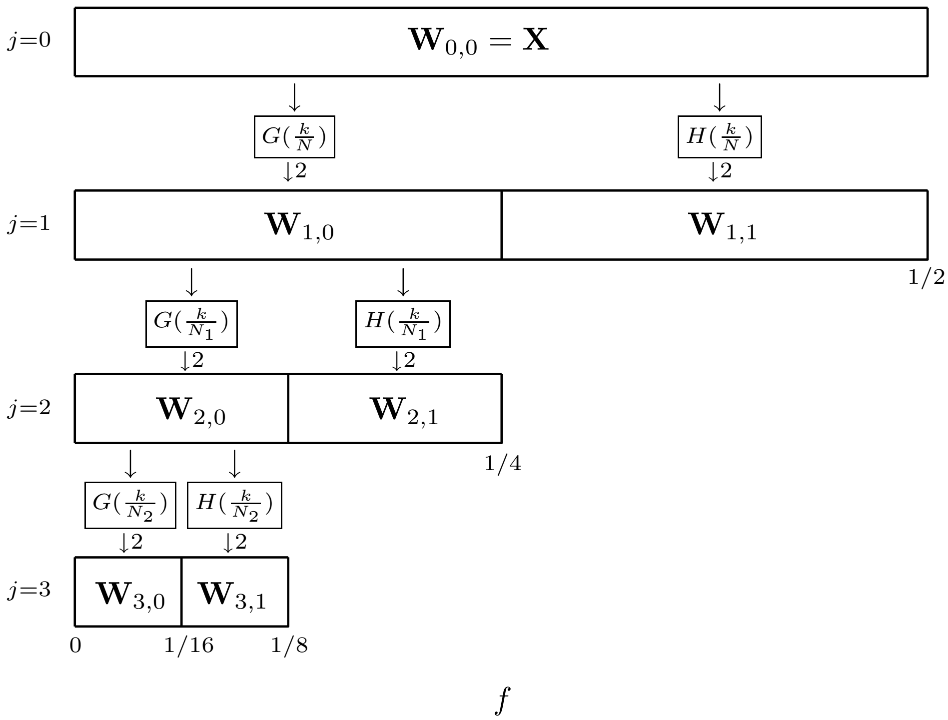

Figure 12. Flow diagram illustrating the analysis of $\mathbf{X}$ into $\mathbf{W}_{3,0}$, $\mathbf{W}_{3,1}$, $\mathbf{W}_{2,1}$ and $\mathbf{W}_{1,1}$, which is identical to a partial DWT of level $J_0 = 3$.

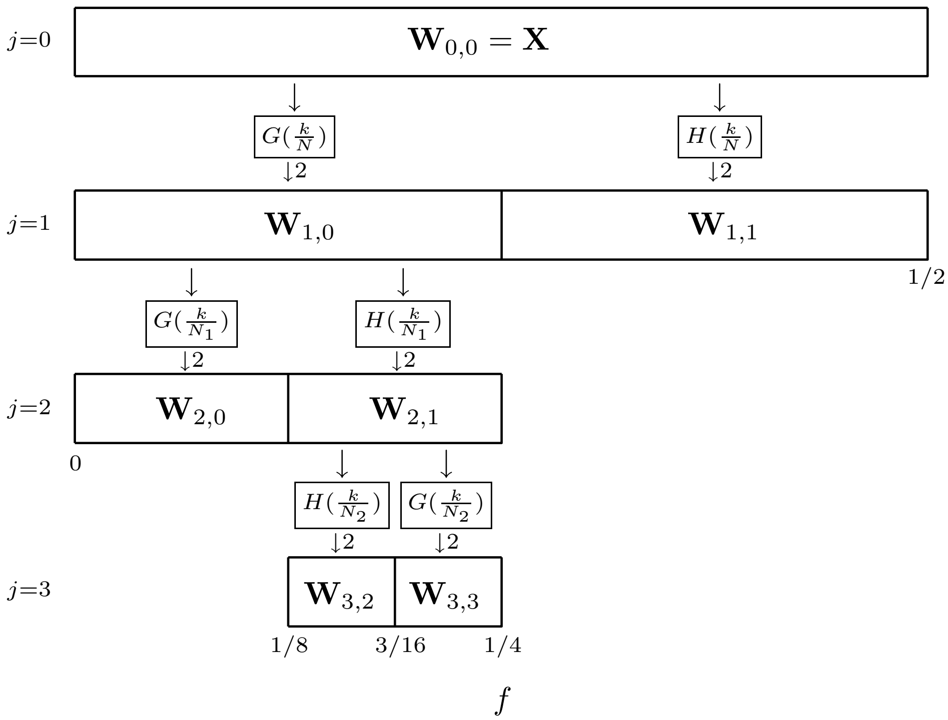

Figure 13. Flow diagram illustrating the analysis of $\mathbf{X}$ into $\mathbf{W}_{2,0}$, $\mathbf{W}_{3,2}$, $\mathbf{W}_{3,3}$ and $\mathbf{W}_{1,1}$, an arbitrary disjoint dyadic decomposition.